A Letters Journal Exploring the Frontiers of Physics

May 2009

EPL, **86** (2009) 37007
doi: 10.1209/0295-5075/86/37007

www.epljournal.org

Impact of an oxygen dopant in $Bi_2Sr_2CaCu_2O_{8+\delta}$

S. Johnston[1,2,3], F. Vernay[4] and T. P. Devereaux[2,3(a)]

[1] *Department of Physics, University of Waterloo - Waterloo, Ontario, N2L 3G1, Canada*
[2] *Stanford Institute for Materials and Energy Sciences, SLAC National Accelerator Laboratory 2575 Sand Hill Road, Menlo Park, CA, 94025, USA*
[3] *Geballe Laboratory for Advanced Materials, Stanford University - Stanford, CA, 94305, USA*
[4] *Paul Scherrer Institut, Condensed Matter Theory Group - Villigen PSI, Switzerland*

received 27 December 2008; accepted in final form 8 April 2009
published online 22 May 2009

PACS 74.62.Dh – Effects of crystal defects, doping and substitution
PACS 71.38.-k – Polarons and electron-phonon interactions
PACS 74.72.Hs – Bi-based cuprates

Abstract – Recent scanning tunneling microscopy studies have shown that local nanoscale pairing inhomogeneities are correlated with interstitial oxygen dopants in $Bi_2Sr_2CaCu_2O_{8+\delta}$. Combining electrostatic and cluster calculations, in this paper the impact of a dopant on the local Madelung and charge transfer energies, magnetic exchange J, Zhang-Rice mobility and interactions with the lattice is investigated. It is found that electrostatic modifications locally increase the charge transfer energy and slightly suppress J. It is further shown that coupling to c-axis phonons is strongly modified near the dopant. The combined effects of electrostatic modifications and coupling to the lattice yield broadened spectral features, reduced charge gap energies and a sizeable local increase of J. This implies a strong local interplay between antiferromagnetism, polarons and superconducting pairing.

The precise role of the atoms lying off the CuO_2 planes has been an intriguing puzzle in the cuprates. While largely thought to provide a charge reservoir to dope holes into the CuO_2 plane, it has become clear that an understanding of the pairing mechanism will require addressing the large variations in T_c arising from the local environment surrounding the CuO_2 planes [1]. Empirically, the role of the apical or axial orbitals has been a vehicle linking T_c either to an effective electron hopping t' along diagonal Cu-Cu bonds [2] or to the stability of the Zhang-Rice singlet (ZRS) [3]. However, to date these arguments have pointed out possible links but offer little microscopic reason for the impact on T_c itself.

Scanning tunneling microscopy (STM) in $Bi_2Sr_2CaCuO_{8+\delta}$ (Bi-2212) has revealed that nanoscopic inhomogeneity is correlated with the location of interstitial oxygen dopant atoms [4] or the superlattice modulation [5]. The location of dopants has been correlated with suppressed peak features with larger gap energies in the observed local density of states (LDOS), and have been associated with local modification of superconducting pairing [6]. This suggests a non-trivial link between the dopant atoms and the electronic properties of the material on a local level.

In metallic systems, such defects can be effectively screened and have little impact on the electrostatics of the material. This is in contrast to the cuprates, which have poor screening along the c-axis and are unable to effectively screen the dopant's impurity charge. As a result, these dopants and accompanying structural changes may have a substantial impact on the electrostatic properties of the material. This may be reflected in quantities such as the charge transfer energy Δ, effective hoppings t, t', magnetic exchange interaction J, or electron-phonon (el-ph) coupling strength λ.

From t-J studies [7], it has been argued that dopants give an enhancement of J and thus larger gap energies if one assumes a dominant spin-fluctuation-based pairing mechanism. While the overall pairing mechanism —Coulomb repulsion, magnons, phonons, or some combinations of each— is still a subject of intense debate, the overall shape of the observed LDOS suggests that incoherence, giving broad spectral features, is an important ingredient to understand local pairing modifications.

In order to quantitatively address these issues, electrostatic Ewald calculations are performed for Bi-2212

(a) E-mail: tpd@stanford.edu

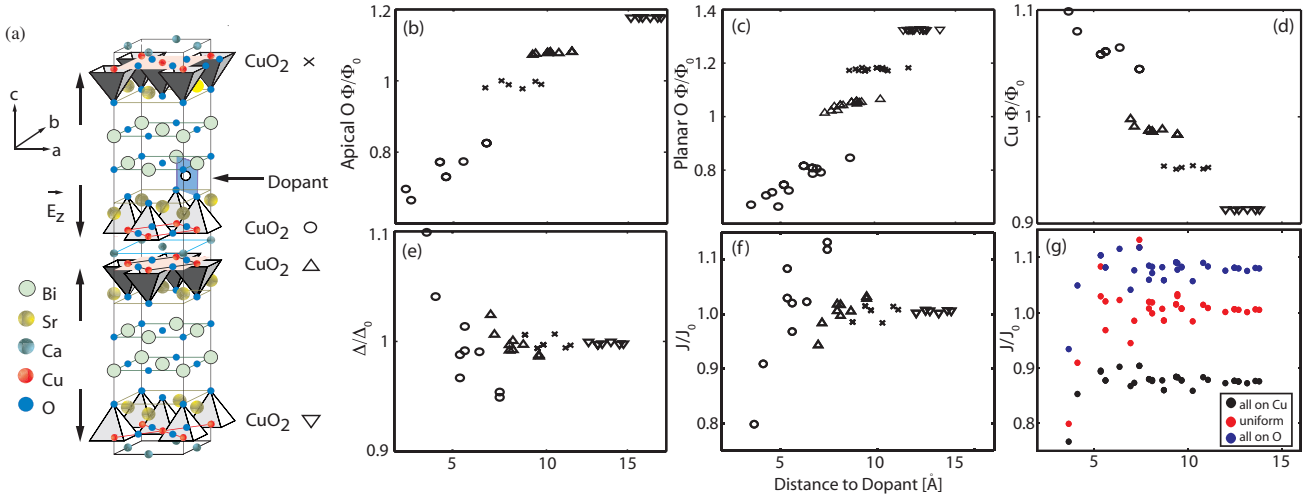

Fig. 1: (Colour on-line) (a) Schematic location of the dopant oxygen in Bi-2212 unit cell. Individual CuO_2 planes are labelled by the symbols shown. The arrows on the left indicate the orientation of the local oxygen crystal fields for the undoped lattice. (b–d) Madelung energies of the apical O, planar O and Cu sites, respectively, in the doped lattice. The local value of the charge transfer energy Δ (e) and derived exchange interaction J (f), obtained by averaging $\Delta\Phi_M$ between Cu and its four neighbouring O sites. (g) Resulting J for different distributions of charges. All values have been normalized to the undoped lattice values. The distance to dopant is defined as the distance to the closest dopant, accounting for the periodicity of the superlattice.

supercells to determine the spatial dependence of the Madelung energies around atomic sites in the crystal. It is found that while Madelung energies on O and Cu are spatially varied on the scale of eVs, these changes largely cancel and Δ is slightly increased near the dopant, yielding an overall suppression locally to J. This information is then combined into exact diagonalization (ED) cluster studies, yielding effective parameters t, t', J and J'. Large $O(1)$ changes are found in both t' and c-axis el-ph coupling λ, quantities which are known to strongly modify a $d_{x^2-y^2}$ pairing interaction. Finally, ED cluster studies including c-axis phonons are shown to produce broadened spectra, a reduced charge gap, in agreement with experiments [4]. As a consequence, a sizeable local increase of J results due to reduced gap *via* a gain in lattice energy. While a unique pairing mechanism cannot be determined in our approach, our results imply a strong interplay and entanglement between el-ph coupling, local superconducting pairing and antiferromagnetic correlations.

The Ewald summation technique [8] is a powerful technique for evaluating sums of long-ranged electrostatic interactions. In essence, it breaks the summation into two pieces; a well-behaved short-ranged piece plus the problematic long-ranged piece. The short-ranged piece is easily evaluated in real space, while the long-ranged piece is evaluated in reciprocal space where it becomes short-ranged and rapidly convergent. Electrostatic calculations using Ewald's method are performed on a supercell consisting of $3\times3\times1$ Bi-2212 unit cells and containing 270 atoms. We have examined supercells four times this size and found that the results are not qualitatively different. Each unit cell contains two primitive cells stacked along the c-axis for a total of four CuO_2 planes, as shown in fig. 1(a). Using formal valences for the atoms along with the known structural data [9], the Madelung energies Φ obtained are $\Phi_{apex,plane} = 18.48,\ 10.16\,\text{eV}$ for the apical, planar oxygen sites, respectively, and $\Phi_{\text{Cu}} = -38.22\,\text{eV}$ for the copper site, consistent with the values reported previously [3]. The charge transfer Δ is related to the difference in Madelung energies for the Cu and O sites, $\Delta\Phi_M = \Phi_{\text{O}} - \Phi_{\text{Cu}}$ and is given by

$$\Delta = \frac{\Delta\Phi_M}{\epsilon(\infty)} - I_{\text{Cu}}(2) + A_{\text{O}}(2) - \frac{e^2}{d_p}, \qquad (1)$$

where $I_{\text{Cu}}(2)$ and $A_{\text{O}}(2)$ are the second ionization and electron affinity energies for the Cu and O sites, respectively. The factor of e^2/d represents the contribution of the Coulomb interaction between the introduced electron-hole pair. In this work, we take the dielectric constant $\epsilon(\infty) = 3.5$ and $I_{\text{Cu}}(2) - A_{\text{O}}(2) + e^2/d = 10.9\,\text{eV}$ [3], yielding $\Delta = 2.92\,\text{eV}$. Besides setting the energy scale for gap excitations, Δ largely governs the magnetic exchange energy J. Using a canonical standard set of parameters in the limit of small hole hopping[1] [10], an exchange energy $J \sim 147\,\text{meV}$ is obtained, in rough agreement with experiments [11].

The Ewald calculation was then repeated with a single oxygen dopant atom inserted into the unit cell, shown schematically in fig. 1(a), and the neighbouring atoms displaced as indicated from recent LDA studies [12]. The

[1] (In eV): $U_{dd} = 8.8$, $U_{pp} = 4.1$, $t_{pd} = 1.0$, $t_{pp} = 0.5$, $\epsilon_d = 0$ and $\epsilon_p = 2.92$, where U_{pp} and U_{dd} are the on-site Coulomb repulsion for the O $2p$ and Cu $3d_{x^2-y^2}$ orbitals, t_{pd} their overlap, and t_{pp} is the O $2p$-$2p$ overlap integral.

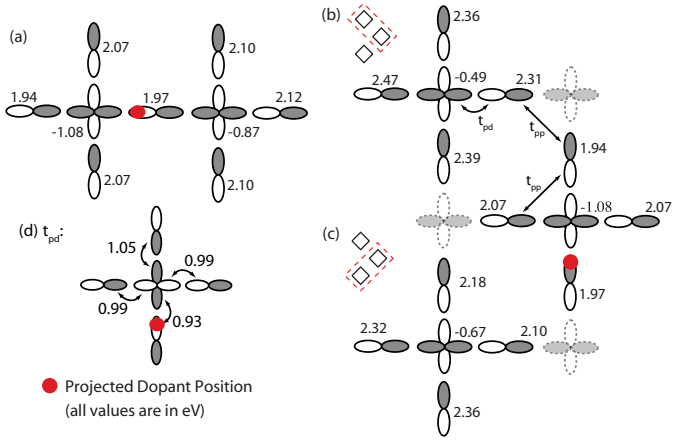

Fig. 2: (Colour on-line) (a) Cu_2O_7 cluster used to extract t and J. (b, c) Two Cu_2O_8 clusters shown in red outline used to extract t' and J'. The values for $\epsilon_{\rm p,d}$ are indicated. (d) Modifications to $t_{\rm pd}$ due to the dopant induced displacements.

oxygen dopant was assigned formal valence, with surplus charge distributed equally among orbitals in the closest CuO_2 planes.

The site-dependent Madelung energies are presented in fig. 1(b)–(d), showing large scale variations for sites closest to the dopant atom. Suppressions/enhancements of O/Cu Madelung energies are observed, respectively, rising/falling to bulk values, shifted by the presence of doped holes, further away from the dopant. However, since the relative sign of the Madelung energies for Cu and O are negative, these changes largely cancel for $\Delta\Phi_M$ and thus Δ (fig. 1(e)) is largely unaffected.

Modifications in Δ allow us to examine the effect of the dopant on the exchange energy J (fig. 1(f)). Reflecting the spatial variations of Δ, J is suppressed by up to 20% near the dopant. Allocating dopant excess charge on either Cu or O, or distributed on both result in slightly different values of J (fig. 1(g)) but the overall suppression seems rather immune to the way in which charge is distributed.

To test this in a non-perturbative way, ED studies of three-hole Cu_2O_7 (fig. 2(a)) and Cu_2O_8 (fig. 2(b) and (c)) clusters were employed to determine changes to the ZRS parameters [13]. Including Cu $3d_{x^2-y^2}$, O $2p_x$ and $2p_y$ orbitals, the Hamiltonian is $H = \sum_{i,\sigma} H_{i,\sigma}$, where

$$\begin{aligned} H_{i,\sigma} \;=\; & \epsilon_d^i d_{i,\sigma}^\dagger d_{i,\sigma} + \sum_\delta \epsilon_p^{i,\delta} p_{i,\delta,\sigma}^\dagger p_{i,\delta,\sigma} \\ & + \sum_\delta t_{pd}^{i,\delta} [d_{i,\sigma}^\dagger p_{i,\delta,\sigma} + \text{h.c.}] + \sum_{\delta\neq\delta'} t_{pp}^{\delta,\delta'} p_{i,\delta,\sigma}^\dagger p_{i,\delta',\sigma} \\ & + U_{dd} \hat{n}_{i,\uparrow}\hat{n}_{i,\downarrow} + U_{pp} \sum_\delta \hat{n}_{i,\delta,\uparrow}\hat{n}_{i,\delta,\downarrow}, \end{aligned} \tag{2}$$

where δ denotes the Cu-O basis vectors and $\hat{n}$ the number operator. From this three-band model, an effective single-band Hubbard or t-J model is derived, with effective nearest $2t$ and next-nearest $2t'$ neighbour hoppings determined from the bonding-antibonding splitting of the ZRS, and J derived from singlet-triplet splitting. In terms of clusters, Cu_2O_7 determines t and J as the ZRS involves a common bridging oxygen while Cu_2O_8 clusters yield t', J'*via* O-O hopping [13]. For the undoped lattice, $t = 330$, $t' = -140$ meV and antiferromagnetic exchange couplings of $J = 158$, $J' = 14.4$ meV are characteristically obtained. J may be further fine-tuned by adjusting t_{pd} and t_{pp}.

The dopant is included by locally varying the on-site Cu and O energies ϵ_d and ϵ_p, respectively, shown in fig. 2. Here, two Cu_2O_8 clusters are used which differ with respect to the location of the dopant, and the site energies have been determined from site modified Madelung energies (fig. 1), according to eq. (1). For the Cu_2O_7 cluster, $t = 336$ and $J = 155$ meV are obtained, while for the two Cu_2O_8 clusters (fig. 2(b) and (c)) we obtain $t' = -187(-237)$ meV and $J' = 15(15)$, respectively. Electrostatic modifications to J and J' are slightly suppressed over undoped cluster values, in general agreement with Madelung estimates, although the magnitude is smaller. Importantly, we note that the symmetric placement of the dopant for the Cu_2O_7 cluster gives only small changes to t, while for Cu_2O_8 the increases are noticeably larger, particularly for geometry fig. 2(b) compared to fig. 2(c). The asymmetric location of the dopant favours occupation of the oxygen ligand orbitals in the plaquette containing the dopant, giving larger modification of t'.

We have repeated these cluster calculations, including the modulations in $t_{\rm pd}$ induced by the structural distortions, according to the LDA displacements of Cu-O bond distances [12,14], shown in fig. 2(d), and obtain $t = 324$, $J = 142$, $t' = -180(-234)$ and $J' = 17(19)$ meV. This tends to further suppress J. Thus, oxygen dopant's net effect is to mildly suppress J and increase t', indicating that the dopant cannot be viewed as only modifying site energies and increasing J in downfolded single-band models [7]. This is also supported by recent perturbation examinations of J due to local variations in band structure [15].

In addition, we have investigated the attractive or repulsive effect of the dopant on local ZRS binding energy. When examining the ground state energy of the three hole clusters in the presence of the dopant, the ground state is lowered on these small clusters by the dopant and therefore may attract local hole charge density. We found that the dopant alters the ZRS density for the Cu_2O_7 cluster, attracting 10% more weight in the plaquette nearest to the dopant. Part of this charge reorganization will of course be screened by the long-range Coulomb interactions and carrier metallicity which will tend to minimize charge density variations, and will also be compensated by charges in the overall chemical potential in the grand canonical ensemble. Thus, while this would be better studied in larger clusters, we infer that the changes by the dopant to the local ZRS properties t, J and t', J' seem to represent the most dominant effects on the local bandstructure. This remains a topic of future interest.

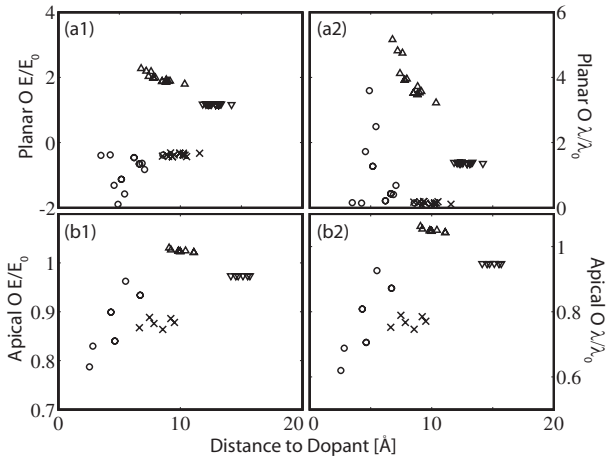

Fig. 3: (a1, b1) Normalized local crystal fields at the planar and apical oxygen sites of the doped lattice. (a2, b2) The corresponding electron-phonon coupling strength $\lambda \propto E^2$. The data points follow the same key as fig. 1.

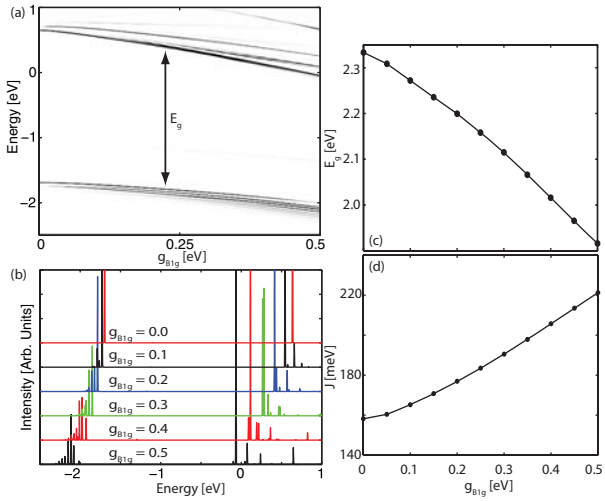

Fig. 4: (Colour on-line) (a) The electron addition and removal spectra obtained from Cu_2O_7 clusters coupled to c-axis oxygen vibrations as a function of el-ph coupling strength $g_{B_{1g}}$. The energy gap E_g is indicated. (b) The electron addition (positive energy) and removal (negative) spectra as a function of energy for selected coupling strengths. (c, d) E_g, J as a function of el-ph coupling, respectively.

Since the Madelung energies are locally modified on the eV scale, real space modifications may result in substantial changes to local crystal fields. Ions vibrating along the c-axis are sensitive to spatial gradients of the Madelung energies, and Devereaux *et al.* [16] has shown that these values of the local field determines the overall strength of el-ph coupling at the oxygen sites, controlling coupling to Raman active A_{1g} planar and apical oxygen vibrations, and out-of-phase planar B_{1g} vibrations. While these couplings themselves are not sufficiently strong to give high T_c's, local changes of el-ph coupling due to eV scale changes in Madelung energies in principle can have a strong impact on local bosonic pairing [17,18], polaron formation, as well as magnetic-based pairing *via* modifications of the overall properties of the ZRS. Therefore, we have examined the dopant's effect on the crystal field in connection to local changes in el-ph coupling.

For the undoped crystal, c-axis crystal fields are $E_{apex,plane} = 18.74,\ 1.16\,\mathrm{eV/\mathring{A}}$ for the apical, planar oxygen sites, respectively, oriented as indicated in fig. 1(a). For the doped lattice, in fig. 3(a1) and (b1) we plot the local c-axis electric field strength at the planar, apical oxygen sites, respectively, and the corresponding el-ph coupling strength λ in fig. 3(a2) and (b2) [16]. One can see that the E-field strength is very sensitive to the local symmetry breaking introduced by the dopant, especially in the case of the planar oxygen atoms. The presence of the dopant's bare charge in the otherwise positively charged SrO/BiO structure suppresses the field in the closest lying plane, and the structural changes further modify the local fields. The largest changes to the E-field occur in the plane whose field is oriented towards the dopant. In this case, the geometry is such that the dopant's bare charge increases the strength of the original field, driving λ for the c-axis planar oxygen modes up by a factor of 5. As it is well known that the c-axis phonons give an attractive interaction in the $d_{x^2-y^2}$ channel, this suggests that superconductivity may be locally promoted by the dopant, in agreement with the assessment of ref. [6]. The enhanced el-ph coupling may on the other hand drive a tendency to locally bind a hole to the lattice near the dopant location. This raises the possibility that LDOS modifications could be related to local polarons rather than pairing.

To address this issue, ED was employed for Cu_2O_7 Hubbard clusters coupled to c-axis oxygen vibrations: $H = H_{el} + H_{lat} + H_{el\text{-}ph}$, where H_{el} is defined in eq. (2), and $H_{lat} = \sum_\nu \Omega_\nu \hat{n}^\nu, \quad H_{el\text{-}ph} = \sum_{\nu,\delta\cdot\sigma} g_\nu (b_\nu^\dagger + b_\nu) e_\nu^\delta p_{\delta,\sigma}^\dagger p_{\delta,\sigma}$. Here $\hat{n}^\nu$ is the phonon number operator for branch ν, e_ν^δ is the polarization of the ν-th quantized local displacement, and $g_\nu = eE\sqrt{\hbar/2M_O\Omega_\nu}$ sets the el-ph coupling strength to mode ν. We consider coupling to uniform out-of-phase B_{1g} and in-phase A_{1g} c-axis modes ($\Omega = 36$ and $55\,\mathrm{meV}$, respectively) coupled to the oxygen hole density by the local field eE. We have not included any local modifications to the phonon mode energies compared to the bulk.

To make contact to STM LDOS, the electron addition, removal spectra $A_\pm$, defined as

$$A_\pm(\omega) = \sum_i |\langle \Psi_i^{1,3} | c, c^\dagger | \Psi_{gs}^2 \rangle|^2 \delta(\omega - E_i^{1,3} + E_{gs}^2), \qquad (3)$$

where Ψ_i^n denotes the n-hole states with energy E_i^n, are plotted in fig. 4(a) and (b) for different values of el-ph coupling $g_{B_{1g}} = \sqrt{55/36} g_{A_{1g}}$. A large number of phonon quanta have been used such that the results are independent of the number of phonons for the parameter region

investigated. As the coupling is increased, the spectral weight is gradually transferred into phonon side bands giving broader and suppressed spectral peaks. The corresponding energy gap E_g between the first removal and addition states *decreases* with increasing $g_{B_{1g}}$ (fig. 4(c)) as the effective charge transfer energy is reduced by the gain in lattice energy. As a consequence, the value of J (correspondingly determined from two-hole Cu_2O_7 clusters with phonons) increases substantially with increasing $g_{B_{1g}}$, as shown in fig. 4(d). The decrease of E_g and increase of J due to local phonons will overwhelm the countering effects from purely electrostatic considerations as the coupling to the lattice increases.

To estimate the size of the effect for Bi-2212, $E_{plane} = 1.16\,\text{eV}$ for the undoped lattice yields $g_{B_{1g}} \sim 0.073\,\text{eV}$, well into the large polaron regime where side bands are weak. Near the dopant, however, $g_{B_{1g}}$ is enhanced to $\sim 0.2\,\text{eV}$, where side bands begin to develop spectral weight in the removal/addition spectra and the charge gap is reduced (fig. 4(a)–(c)). At the same time, for this parameter regime, which is characteristic of multilayer cuprates, J is increased by 20 meV, much greater than the small reduction determined from electrostatic effects alone. Thus for realistic parameter regimes, c-axis phonons act in concert with strong spatial variations of Madelung energies giving an increase in J as well. The dopant may then provide two coupled channels for d-wave pair enhancement, while causing suppressed spectral features as a consequence of strong local el-ph coupling. This is qualitatively what has been observed in the experiments [4]. Such synergy among phonons, polarons and antiferromagnetism has been already noticed in cluster quantum Monte Carlo studies [19].

In summary, we have investigated electrostatic modulations of local Madelung energies arising from the presence of a dopant atom in Bi-2212 unit cells. While eV changes are found for the Madelung energies for copper and oxygen, these changes largely cancel for the charge transfer energy and give small local suppression to J. However, the strong local variations in Madelung energies are manifest in order-1 changes in el-ph coupling for c-axis oxygen modes. Using cluster studies, it was found that in combination, electrostatic modifications and coupling to the lattice yield broadened spectral features, reduced charge gap energies E_g and a sizeable local increase of J, implying a strong local interplay between antiferromagnetism, polarons and superconducting pairing. The amount of variation of the local charge gap can thus serve as an important diagnostic for determining lattice coupling, electrostatic effects and pairing. It is an open question whether a link between these quantities can be made experimentally.

* * *

The authors would like to acknowledge valuable discussions with A. Balatsky, J. C. Davis, W. Harrison, P. J. Hirschfeld, H.-P. Cheng, K. McElroy, B. Moritz and J.-X. Zhu, and would like to thank the Pacific Institute for Theoretical Physics, where part of this work was performed. Work is supported in part by the US Department of Energy under contract No. DE-AC02-76SF00515 and NSERC.

REFERENCES

[1] Eisaki H. *et al.*, *Phys. Rev. B*, **69** (2004) 064512.
[2] Pavarini E. *et al.*, *Phys. Rev. Lett.*, **87** (2001) 047003.
[3] Ohta Y., Tohyama T. and Maekawa S., *Phys. Rev. B*, **43** (1991) 2968.
[4] McElroy K. *et al.*, *Science*, **309** (2005) 1048.
[5] Slezak J. A. *et al.*, *Proc. Natl. Acad. Sci. U.S.A.*, **105** (2008) 3203; Andersen B. M. *et al.*, *Phys. Rev. B*, **76** (2007) 020507.
[6] Nunner T. S. *et al.*, *Phys. Rev. Lett.*, **95** (2005) 177003; Mori M. *et al.*, arXiv:0805.1281.
[7] Zhu J.-X., cond-mat/0508646; Maśka M. M. *et al.*, *Phys. Rev. Lett.*, **99** (2007) 147006.
[8] Ewald P., *Ann. Phys. (N.Y.)*, **369** (1921) 253.
[9] Kovaleva N. N. *et al.*, *Phys. Rev. B*, **69** (2004) 54511.
[10] Eskes H. and Jefferson J. H., *Phys. Rev. B*, **48** (1993) 9788.
[11] Devereaux T. P. and Hackl R., *Rev. Mod. Phys.*, **79** (2007) 175.
[12] He Y. *et al.*, *Phys. Rev. Lett.*, **96** (2006) 197002.
[13] Eskes H. and Sawatzky G., *Phys. Rev. B*, **43** (1991) 119.
[14] Harrison W. A., *Elementary Electronic Structure* (World Scientific) 2004.
[15] Foyevtsova K., Valenti R. and Hirschfeld P. J., arXiv:0809.2919.
[16] Devereaux T. P. *et al.*, *Phys. Rev. B*, **59** (1999) 14618.
[17] Balatsky A. V. and Jian-Xin Zhu, *Phys. Rev. B*, **74** (2006) 094517; Jian-Xin Zhu *et al.*, *Phys. Rev. Lett.*, **97** (2006) 177001; *Phys. Rev. B*, **73** (2006) 014511.
[18] Lee J. *et al.*, *Nature (London)*, **442** (2006) 546.
[19] Macridin A. *et al.*, *Phys. Rev. Lett.*, **97** (2006) 056402.